Polymer Chemistry

ROYAL SOCIETY OF CHEMISTRY

REVIEW

View Article Online
View Journal | View Issue

Cite this: *Polym. Chem.*, 2021, **12**, 1347

Quinoidal conjugated polymers with open-shell character

Xiaozhou Ji and Lei Fang *

Received 11th September 2020,
Accepted 4th February 2021

DOI: 10.1039/d0py01298j

rsc.li/polymers

π-Conjugated polymers composed of quinoidal or proquinoidal building blocks represent an intriguing class of macromolecules in terms of both fundamental research and practical applications. They have received increasing research interest in recent years on account of their distinct structural features and unique properties including open-shell electronic configurations and delocalization of polarons. Investigations of the influences of the quinoidal character on optical, electronic, and magnetic properties demonstrated a great prospect of these polymers in diverse application fields. This review summarizes the recent development of quinoidal conjugated polymers with regard to design, synthesis, fundamental properties, and representative applications, with emphasis on their open-shell character and high-spin materials properties. The challenges and outlook associated with this research field are also discussed.

1. Introduction

1.1 Quinoidal character of π-conjugated systems

An organic π-conjugated system is a molecular entity featuring side-to-side interactions of p-orbitals across intervening σ-bonds, typically in the form of alternating single and multiple bonds.[1] π-Conjugated polymers have been investigated extensively and employed in a wide range of applications on account of their intriguing electronic and optical properties. Most conjugated polymers contain cyclic π-units in the main chain. These building blocks can be represented by either a Hückle aromatic form or a "quinoidal" form. In the aromatic form, the aromatic (poly)cyclic building blocks are typically connected with one another by single bonds. In contrast, in the quinoidal form, a π-unit exerts no local ring aromaticity and is typically connected with others by double bonds. An aromatic π-conjugated unit can also be described as "proquinoidal" if it possesses a significant resonance contribution from the quinoidal form. Herein, we use the term "quinoidal

Department of Chemistry, Texas A&M University, College Station, TX 77843-3255, USA. E-mail: fang@chem.tamu.edu

Xiaozhou Ji

Xiaozhou Ji received her BS degree from Nanjing University in 2015. In the same year, she joined the group of Dr Lei Fang at Texas A&M University, where she received her PhD degree in chemistry. In 2021, she joined Dr Zhenan Bao's group at Stanford University as a postdoctoral scholar. Her research interests include conjugated molecules and macromolecules, quinoidal π-systems, and doping of organic materials.

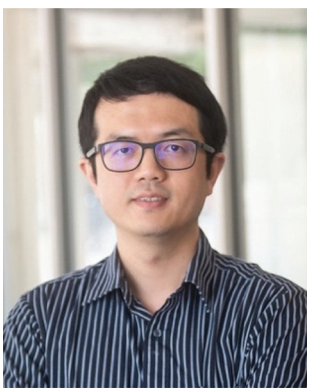

Lei Fang

Lei Fang is an associate professor in the Department of Chemistry at Texas A&M University. He obtained his BS (2003) and MS (2006) degrees from Wuhan University. He began his PhD study at the University of California Los Angeles, and received the degree from Northwestern University in 2010, mentored by Professor Sir Fraser Stoddart. Subsequently, he spent two and a half years at Stanford University as a postdoctoral scholar working with Professor Zhenan Bao. In 2013, he joined the faculty of Texas A&M University, where he currently leads a multidisciplinary research team focusing on functional organic materials.

conjugated polymer" to describe conjugated polymers that exhibit significant quinoidal character due to the presence of quinoidal or proquinoidal building blocks in the backbone. Quinoidal conjugated polymers often exhibit drastically different structural features, such as bond lengths, conformation, open-shell character, *etc.*, compared to their counterparts composed of non-quinoidal aromatic units. Consequently, they can exhibit distinctive electronic, optical, and magnetic properties that are often not accessible in aromatic conjugated polymers, promising for a wide range of intriguing applications.

For a certain π-system, the degree or ratio of the quinoidal character, with respect to the aromatic character, can be conveniently quantified using the parameter bond length alternation (BLA), which is defined as the average of the differences in bond lengths between the alternant single and double bonds.[2] As an important structural parameter, BLA is related to the electronic properties of a conjugated polymer, such as the bandgap energy [the energy difference between the highest occupied molecular orbital (HOMO) and the lowest unoccupied molecular orbital (LUMO)]. To illustrate these concepts, here we take one of the simplest conjugated polymers—polyacetylene (Fig. 1a)—as an example. Ideally, an infinite polyacetylene chain with equal length alternant bonds (zero BLA) possesses the largest π-conjugation, exhibiting zero bandgap energy and metallic properties. Such a metallic state, however, is unstable. Therefore, Peierls distortion takes place to afford two stabilized degenerate forms with |BLA| > 0. As a result, polyacetylene possesses a non-zero energy bandgap and is non-metallic in reality. For an infinite chain of a conjugated polymer constituted by cyclic aromatic π-units, such as poly-*para*-phenylene (PPP) (Fig. 1b), polythiophene, or polypyrrole, *etc.*, the potential energy curve of the ground state possesses two minima, corresponding to the quinoidal and aromatic forms, respectively. In Fig. 1, BLA is defined as $(d_2 - d_1)/2$ as labeled on the structure; therefore, the quinoidal form shows a negative BLA value while the aromatic form exhibits a positive BLA value.[3] Peierls stabilization contributes to both minima, while the aromatic form is more favorable than the quinoidal form due to the additional stability imparted by Hückle aromaticity, and thus is typically representative of the polymer ground state. To transform between the quinoidal and aromatic forms, the system would go through a high-energy point at which BLA is close to zero on the potential energy curve. The quinoidal character and hence the BLA are closely related to the bandgap energy of π-conjugated systems.[4] In a pioneering study by Brédas, BLA was used as an indicator of the quinoidal character of PPP, polypyrrole, and polythiophene and the calculated bandgaps decrease linearly with increasing quinoidal character.[5] In some recent computational study, the correlation between the quinoidal character and bandgaps of conjugated copolymers was explored with new quantum chemical descriptors that possess higher compatibility and universality than the simple BLA parameter.[6,7]

Apart from BLA, the backbone conformations are often different between a quinoidal conjugated polymer and its aromatic analogue.[9] On account of the double-bond connections between cyclic π-units, a quinoidal structure often exhibits higher coplanarity and rigidity, while its aromatic counterpart possesses a higher degree of freedom for torsional rotation about the single bond linkages.[10] The coplanarity of the quinoidal structure further facilitates electron delocalization throughout the π-system, contributing to a more extended π-conjugation scale.

1.2 Open-shell character of quinoidal structures

The past four decades have witnessed increasing research interest in quinoidal small molecules and oligomers. The resonance between the closed-shell and open-shell forms of quinoidal molecules has been studied extensively, providing advanced fundamental understanding of the nature of molecular orbitals and spin–spin interactions in these systems.[11] Their electronic, optical, and magnetic properties also show promising potential to be applied in organic electronics and spintronics.[12–16] Quinoidal molecules with open-shell diradical character are also good candidates for singlet fission processes, which play an important role in the latest development of organic photovoltaic applications.[17,18] Related literature reports on small molecules and oligomers have already been summarized in several reviews and accounts.[11,15,19–22] Similar to quinoidal small molecules and oligomers, the open-shell diradical character and spin-active states can be derived from quinoidal building blocks in conjugated polymers.[11,23] In this article, we focus on quinoidal conjugated polymers with open-shell character.

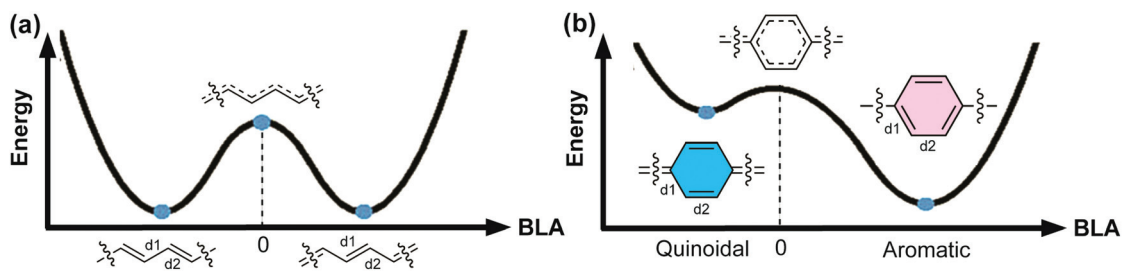

Fig. 1 Energy diagrams of the ground states of the infinite chain of (a) polyacetylene and (b) poly-*para*-phenylene (PPP) as a function of BLA, which is defined as $(d_2 - d_1)/2$. Reproduced (adapted) from ref. 8 with permission from John Wiley and Sons.

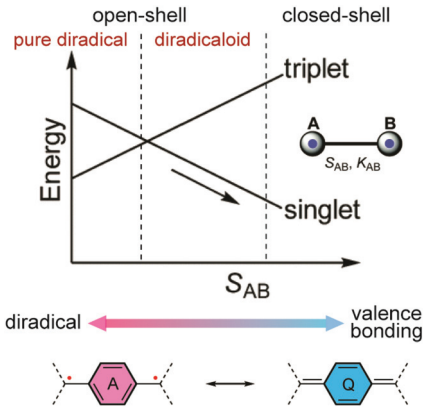

Fig. 2 Change of energies of triplet and singlet electron pairs with the increase in the one-electron overlap integral S_{AB} and resonances between open-shell diradical and closed-shell quinoidal structures. Reproduced (adapted) from ref. 11 with permission from the Royal Society of Chemistry.

From the perspective of resonance forms, the open-shell diradical character of a quinoidal π-system can be considered as a result of the increased resonance contribution of the diradical form due to the stabilization effect of the original quinoidal ring gaining Hückle aromaticity.[24,25] In the energy diagram (Fig. 2), with increasing one-electron overlap integral S_{AB} between two localized orbitals, the singlet molecular orbital is stabilized while the triplet state energy increases, resulting in the progress from open-shell to closed-shell. The energy gap between the singlet and triplet states also changes depending on S_{AB}, leading to varied electronic and magnetic properties. We would like to point out that for quinoidal small molecules and oligomers with defined end groups, the preference of resonance contributions can be critically impacted by the end groups. The impact of end groups in a longer polymeric system, however, is diluted as the molecular weight increases, and the open-shell character is analyzed mainly within the repeating units. Overall, the underlying diradical character often plays an essential role in governing the electronic and magnetic properties of many quinoidal conjugated polymers.

1.3 Quinoidal polarons/bipolarons in doped conjugated systems

Doped π-conjugated polymers are important organic materials that often exhibit open-shell, high-spin properties. Upon redox doping, electrons are injected into/removed from the neutral polymers, leading to anionic/cationic charged segments. In this process, the aromatic building blocks are partially converted into the quinoidal form, thereby affording drastically changed chemical, electronic, and magnetic properties. For example, without doping, polypyrrole or polythiophene is in a dominant aromatic form (Fig. 3a). The energy gap between the overall π-bonding and π*-antibonding orbitals, corresponding to the valence and conduction bands, respectively, renders semiconducting properties.[26] Upon oxidative doping, positive charges are created and local reorganization leads to an ionized quinoidal form. In the solid state, the lattice deformation with a radical cation is termed as a "polaron", whose energy levels are localized in the forbidden band, leading to a simultaneous shift in the Fermi level and electrical conductivity. At a higher doping level, radical cations in close proximity can combine so that the two neighboring positive charges are coupled in the quinoidal unit.[27] Such a doubly-charged quinoidal section can be considered as a "bipolaron" that delocalizes over several rings. In this case, two localized states form in the original bandgap and evolve into two bipolaron bands with increased doping levels. In doped polymers, both high-spin polarons and spinless bipolarons are charge carriers. The low effective mass of polarons and bipolarons and high carrier mobility give rise to the high electrical conductivity of polymers with quinoidal segments,[28] while a study on doped poly(3-hexylthiophene) suggested[29] that polarons possess higher mobility than bipolarons. Polyaniline is another representative conducting polymer material that can be doped into a quinoidal form. Half-oxidation of the neutral polyaniline affords the quinoidal bipolaron structure, which has been proposed to dissociate into polarons and further delocalize into the polaron lattice, rendering high electrical conductivity (Fig. 3b).[30,31] Overall, the quinoidal form is ubiquitous in the doping process of conjugated polymers, and plays an important role in the generation of polarons and bipolarons for the electrical conductivity of conducting polymers.

Although the importance of the quinoidal structure has been revealed for a long time, polymeric π-systems composed of quinoidal or proquinoidal building blocks (defined as "quinoidal conjugated polymers" in this article) and the investigations on their open-shell character are less reported due to the challenges associated with their synthesis and stability.[17] Despite these challenges, a number of important advances have been made to further our knowledge on the design and synthesis of such polymers and to deepen our understanding of the quinoidal properties in macromolecules for a wide range of applications. In this review article, the progress throughout recent decades in this field is summarized based on quinoidal conjugated polymers with open-shell character. Emphases are placed on the synthesis, key features of quinoidal structures, and representative applications. In contrast to the well-reviewed quinoidal conjugated polymers with narrowed bandgaps commonly applied in organic field-effect transistors and photovoltaic applications,[32–35] in this paper, we would like to bring attention to the fundamental properties of quinoidal conjugated structures, including open-shell electronic configurations and state delocalization, and their related applications as high-spin materials.

2. Design and synthesis

In this section, we categorize quinoidal conjugated polymers into two types with (1) proquinoidal and (2) quinoidal building blocks. It is worth noting that the first category can be drawn

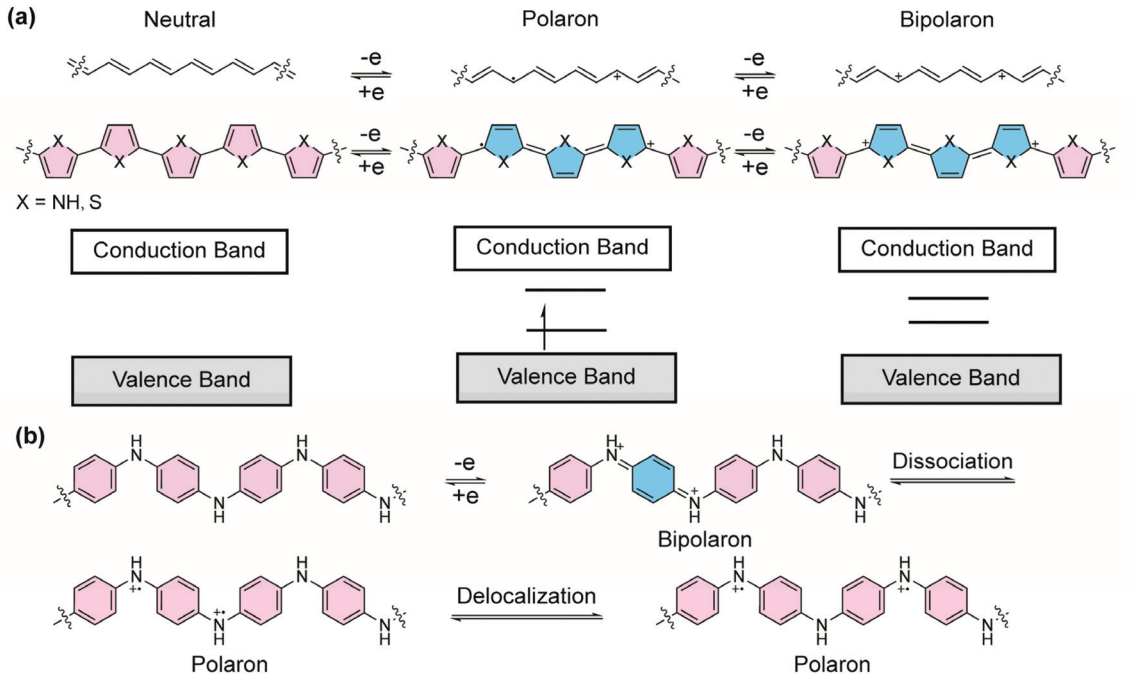

Fig. 3 (a) Graphical illustration of the structures of polyacetylene, polypyrrole, and polythiophene in their undoped form and partially quinoidal form after doping and energy diagrams of the neutral, polaron, and bipolaron states. (b) Polyaniline in the undoped form and doped form with polaron–bipolaron equilibrium.

in fully aromatic formulae in a strict definition. Here they are considered as quinoidal conjugated polymers and are included in this review because of their significant open-shell character and properties associated with their quinoidal resonance forms.

2.1 Proquinoidal polymers

A homopolymer consisting of aromatic yet proquinoidal repeating units is expected to exhibit quinoidal characteristics as a result of the significant contribution of its quinoidal resonance form. Such proquinoidal character can be imparted to the main chain by fusing additional conjugated rings in a way that the aromaticity of the additional rings strengthens the quinoidal contribution of the main-chain units. For example, to render a higher proquinoidal nature in polythiophene, Wudl *et al.* designed and synthesized[36] polyisothianaphthene (PITN). A benzene unit is fused to the 3,4-position of each thiophene repeating unit in the polymer, so that the quinoidal resonance form of the thiophene backbone is augmented by the aromatization of the fused benzene units (Fig. 4a).[37] Compared to conventional polythiophene, PITN exhibits a drastically decreased bandgap energy (~1 eV),[38,39] which is attributed to the increased quinoidal character with smaller BLA according to computational studies.[40] Following this pioneering work, the strategy of imparting the proquinoidal character by fusing an additional aromatic ring has been employed extensively in the synthesis of proquinoidal homopolymers (Fig. 4b). Notable examples include poly(thieno[3,4-*b*]pyrazine),[41–44] poly(thieno[3,4-*b*]thiophene),[45–48] poly(naphtho[2,3-*c*]thiophene),[49,50] poly(dithieno[3,4-*b*:2′,3′-*d*]thiophene),[51] poly(thieno[3,4-*b*]quinoxaline),[50] *etc.* Many of these polythiophene-derived homopolymers were polymerized by electrochemical or chemical oxidation (Fig. 4c).[48] Other methods

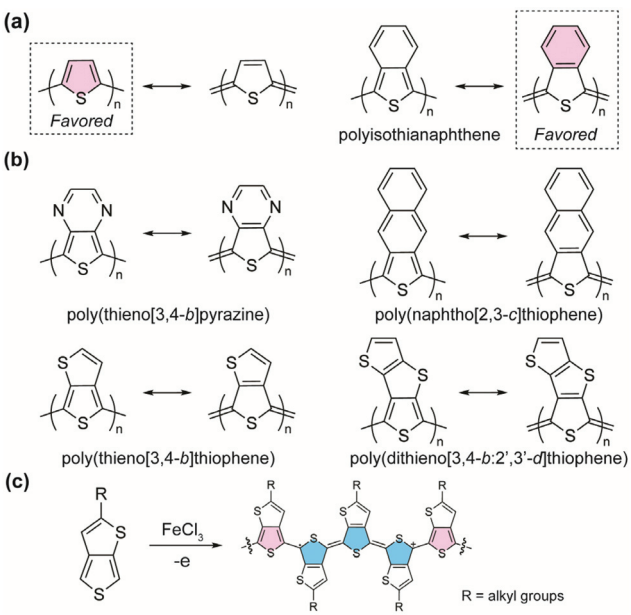

Fig. 4 (a) Resonance structures of polythiophene and polyisothianaphthene; (b) representative examples of proquinoidal homopolymers; (c) oxidation polymerization of thieno[3,4-*b*]thiophene and the doped product with charged quinoidal structures.

have also been reported, such as Grignard metathesis polymerization[43] and nonoxidative polymerization based on phthalide-derived monomers.[52,53] Under oxidative conditions (Fig. 4c), the afforded polymers are in the doped state, containing charged quinoidal structures and featuring narrowed bandgaps and enhanced π-conjugation.

Compared to proquinoidal homopolymers, proquinoidal–aromatic alternating copolymers are much more commonly seen in the recent literature. In such a polymer, one can anticipate a significant resonance proportion in which the proquinoidal unit adopts the quinoidal form. In comparison with aromatic homopolymers, the alternating arrangement of proquinoidal and aromatic building blocks usually generates narrower energy bandgaps. Numerous proquinoidal–aromatic copolymers with proquinoidal building blocks, including thieno[3,4-*b*]pyrazine,[44,54,55] thieno[3,4-*b*]thiophene,[14,56–61] dithieno[3,4-*b*:2′,3′-*d*]thiophene,[62] isothianaphthene,[63] *etc.*, have been developed as active materials for organic field-effect transistors, photovoltaics, organic light-emitting diodes, and many other applications.

In the syntheses of these polymers, Stille coupling polymerization is the most commonly used method to construct copolymers containing alternating proquinoidal and aromatic repeating units (Fig. 5). A number of comprehensive review articles have been published on this topic.[32,33,44,47,64–67] In this context, only several recent representative copolymers with open-shell character are shown here. Benzo[1,2-*d*:4,5-*d*′]bistriazole[68,69] and benzo[1,2-*c*:4,5-*c*′]bis[1,2,5]thiadiazole[70–75] are proquinoidal while electron-accepting building blocks. Conjugated polymers including these two moieties, **P1–4**[78] and **P5** and **P6**,[79] were reported by Tam and Xu. Thiadiazole[3,4-*g*]quinoxaline is another strong proquinoidal acceptor unit and the derived polymers **P7** and **P8** were synthesized by Azoulay.[76,77] The open-shell diradical character of these proquinoidal building blocks leads to appealing conducting properties in their applications.

2.2 Quinoidal–aromatic alternating copolymers

Compared to "proquinoidal" units, "quinoidal" units that adopt a true quinoidal constitution in the ground state are typically less accessible, so that the synthesis of quinoidal–aromatic conjugated polymers requires more careful design to mitigate the stability issue. Two general strategies have been employed for the synthesis: (1) direct polymerization of stabilized quinoidal monomers and (2) post-polymerization modification (*e.g.* oxidation) of an aromatic polymer precursor into its corresponding quinoidal–aromatic form.

Certain quinoidal units derived from thiophenone[78,79] and pyrrolidone[80–83] can be incorporated into conjugated copolymer backbones by Stille coupling polymerization based on monomers with aromatic terminal groups (Fig. 6). Kim's group synthesized copolymers with isatin-terminated indolone quinoidal moieties. Possible *E*- and *Z*-configurational isomers were obtained in thiophene and bithiophene building blocks. When using the 3,4-ethylenedioxythiophene (EDOT)-like repeating units, the noncovalent interactions between sulfur and oxygen atoms lock the conformation of the polymer chain, leading to high coplanarity and stereoregular polymer products. Other quinoidal moieties, such as thieno[2,3-*b*]thiophene and thiophene dioxide, are also designed and synthesized. The afforded copolymers with low energy bandgaps are usually studied in organic field-effect transistor and organic photovoltaic applications. These works have been reviewed in a recent publication.[32] Recently, quinoidal building blocks derived from *para*-aza-quinodimethane were designed and incorporated into copolymers **P9–12** by Liu and coworkers.[84–86] *para*-Quinodimethane is a highly reactive quinoidal moiety with large open-shell diradical character.

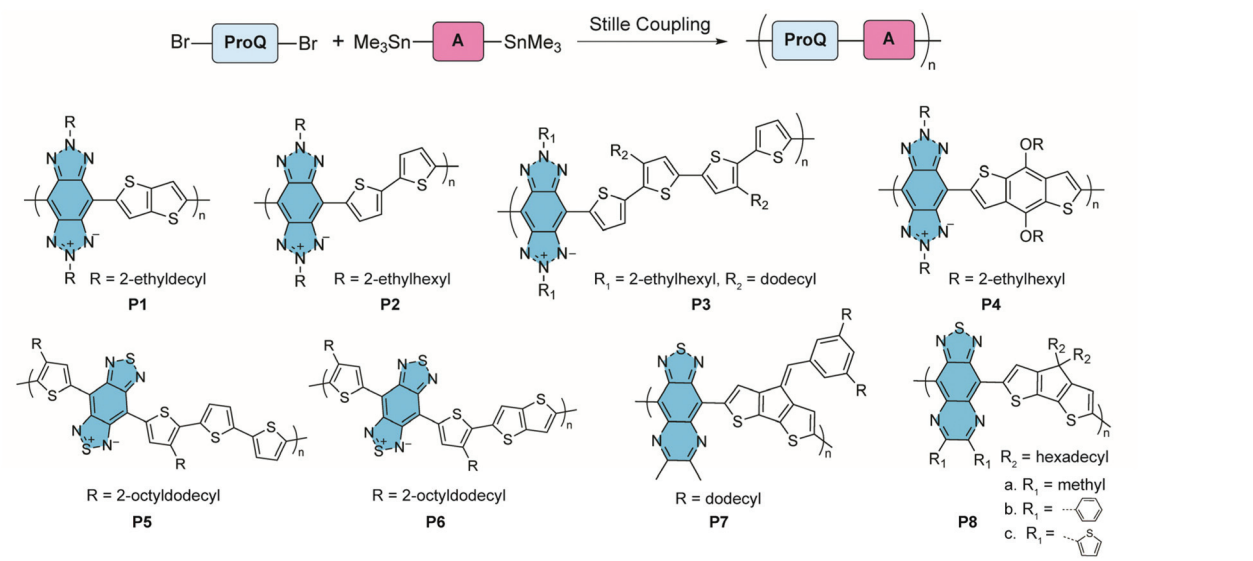

Fig. 5 Synthesis and structural formulae of recently reported proquinoidal–aromatic alternating copolymers demonstrating open-shell character.

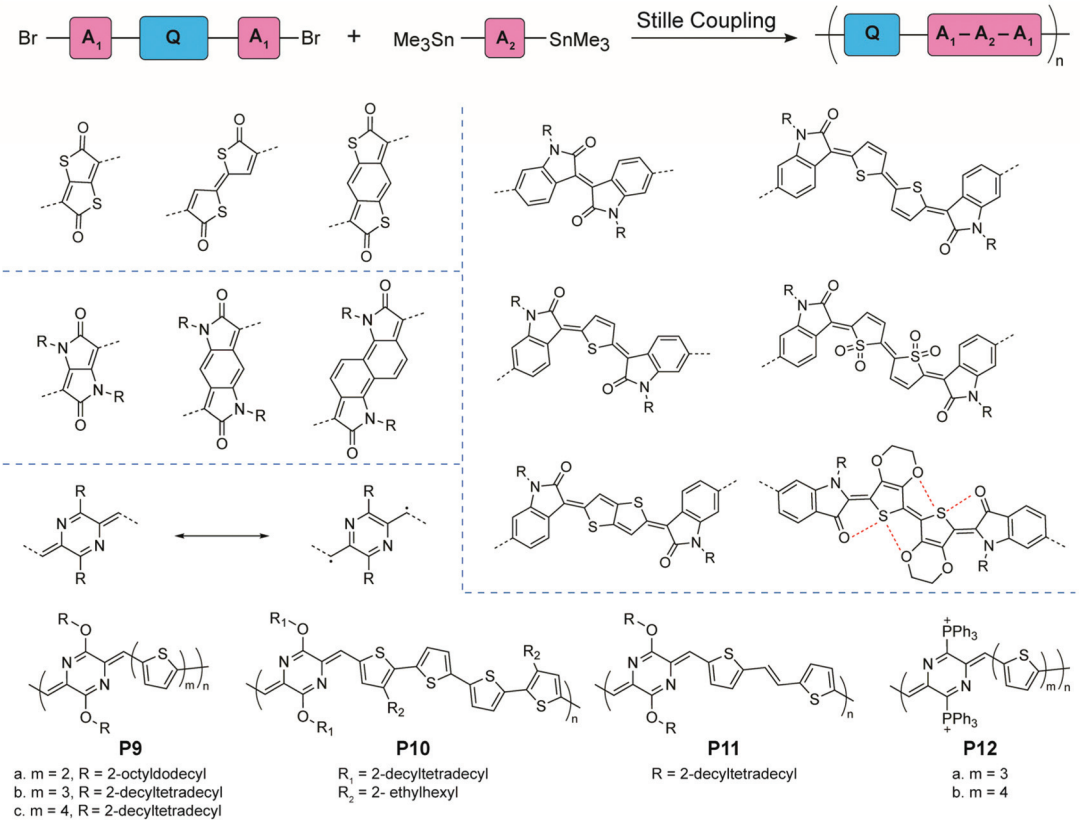

Fig. 6 General synthetic scheme, structural formulae of representative quinoidal building blocks, and structures of *para*-aza-quinodimethane-derived quinoidal–aromatic alternating copolymers.

However, good stability is conferred by introducing heteroatoms into the π-system. The effects of different main-chain building blocks and side chain bulkiness on the film morphology and charge transport were investigated systematically by comparing the **P9** and **P11** series.[84,85] By replacing the ether solubilizing groups with cationic triphenylphosphonium groups, **P12** was obtained as a conjugated polyelectrolyte with reasonable stability and water-solubility.[86]

An alternating quinoidal–aromatic constitution can also be achieved by post-polymerization modification of a fully aromatic precursor. For example, Fang's group designed[87] a series of cyclohexadiene-1,4-diimine-derived, quinoidal–aromatic alternating copolymers featuring a ladder-type constitution (Fig. 7). First, a fully aromatic copolymer is synthesized[88] by polymerizing *para*-diaminophenylene- and fluorene-derived monomers. The ladder-type constitution is subsequently constructed by a ring-annulation reaction, affording **P13a** as a ladder-type analogue of the fully-reduced form of polyaniline (leucoemeraldine). Post-polymerization oxidation converts the *para*-diaminophenylene units into their quinoidal form, namely, cyclohexa-2,5-diene-1,4-diimine units. The partially oxidized polymer **P13b**, as an analogue of an emeraldine base, can be obtained under mild oxidation conditions. The fully-oxidized, alternating quinoidal–aromatic copolymer **P13c** is prepared by peroxide oxidation. The quinoidal structure is confirmed by ^{13}C NMR compared to small molecular models. The redox interconversion between the aromatic form **P13a** and the quinoidal–aromatic form **P13c** is highly reversible thanks to the significantly improved robustness of the π-system imparted by the ladder-type constitution.

Oxidation of methine-bridged polythiophenes represents another interesting strategy for the synthesis of quinoidal–aromatic copolymers (Fig. 8). Chen and Jenekhe synthesized[89] such polymers through a two-step route. First, a thiophene-derived monomer is polymerized with benzaldehyde through an acid-catalyzed Friedel–Crafts reaction. Then the resulting polymer is oxidized to introduce the quinoidal thienomethine moieties in **P14** and **P15**.[90,91] Each quinoidal moiety contains three diastereoisomers, *i.e.*, *E*/*E*, *E*/*Z*, and *Z*/*Z*, leading to isomeric mixtures in the product. In a recent report, a C–C bulk polycondensation reaction was used on the bisthiophene methine monomer, affording **P16** after partial oxidation.[92] Other aromatic building blocks, *e.g.*, diketopyrrolopyrrole, could also be connected with thienoquinodimethane units through Stille coupling polymerization, affording the donor–acceptor copolymer **P17**.[93]

3. Properties and applications

3.1 Open-shell diradical character

The unpaired electrons and their corresponding magnetic moments render intriguing behaviors of quinoidal conjugated

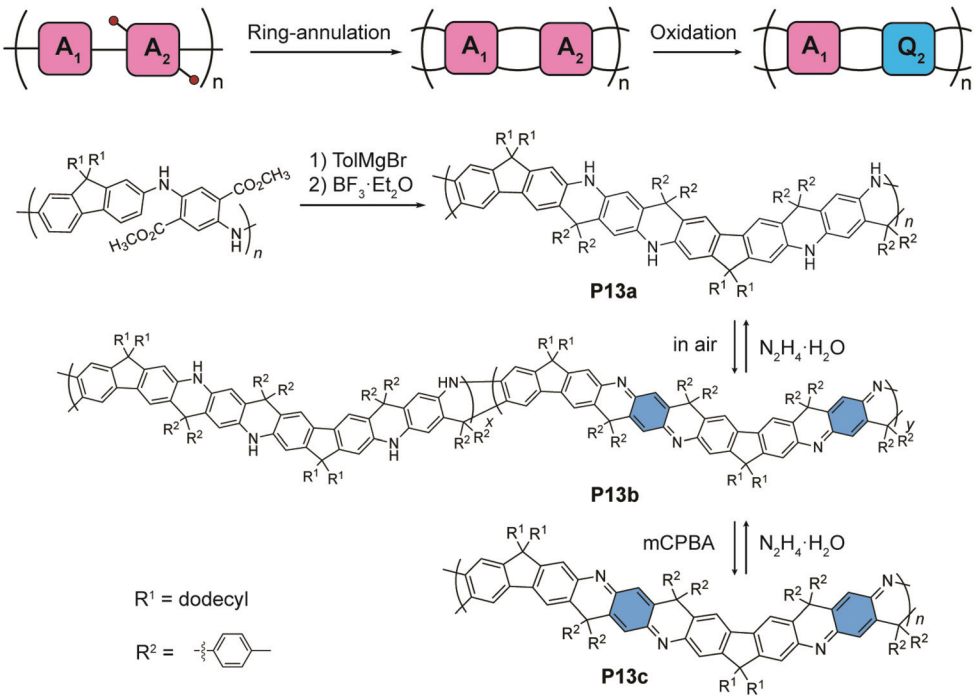

Fig. 7 Synthesis of ladder-type polyaniline derivatives **P13a–P13c**.

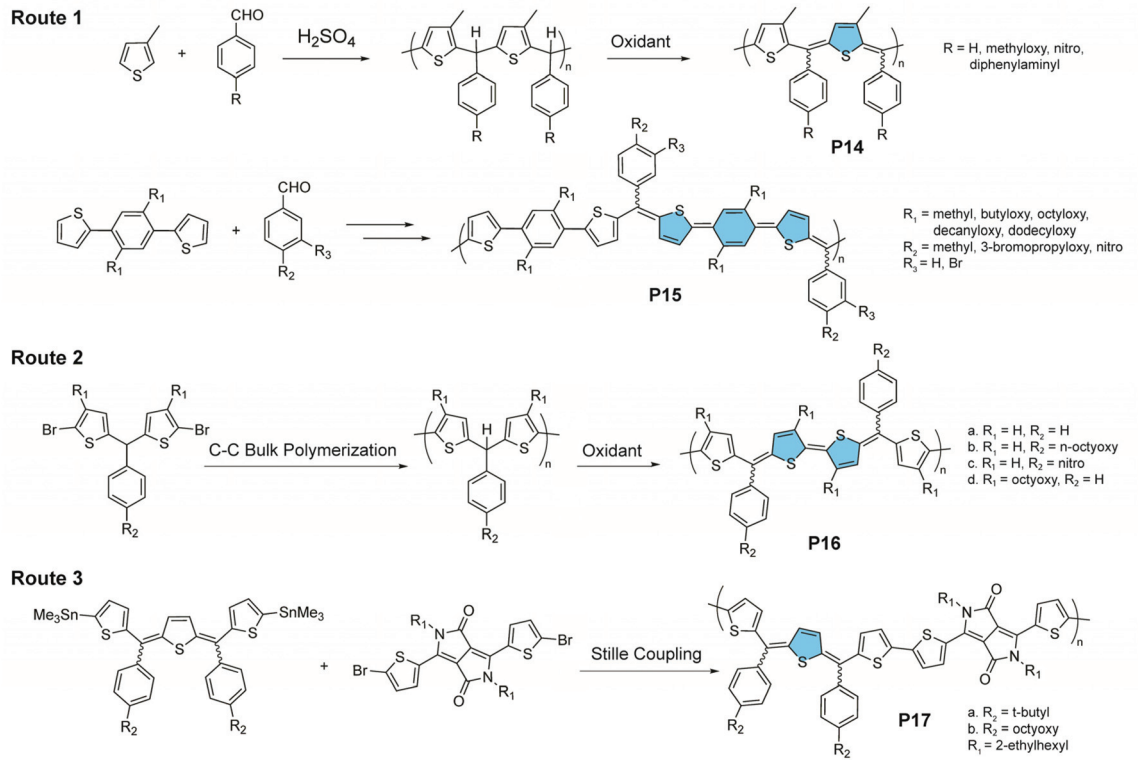

Fig. 8 Three synthetic routes to methine-bridged polythiophenes featuring alternating quinoidal and aromatic units on the main chain.

polymer that are typically not observable on their closed-shell counterparts. Therefore, the investigation of quinoidal polymers with isolable stability of high-spin states has emerged in diverse research fields, on topics of spin manipulation, organic magnetism, quantum functionalities, and interrelated optoelectronic properties.

In proquinoidal–aromatic copolymers such as **P5** and **P6**, the open-shell resonance was characterized, exhibiting increasing electron paramagnetic resonance (EPR) intensities with decreasing temperature, indicating the triplet open-shell ground state (Fig. 9). The smaller temperature dependence of **P5** can be seen as evidence of its larger energy gap between the triplet and singlet states. Magnetic susceptibility χ is a sum of three components: antiferromagnetic coupling between polymer chains (χ_{AFM}), ferromagnetic coupling from the triplet state (χ_{FM}), and temperature-independent paramagnetism arising from coupling between a magnetic ground state and non-thermally populated excited states (χ_{TIP}). The coupling constant of antiferromagnetic coupling J_{AFM} (kcal per mole repeating unit) is calculated to be −0.63 for **P5** and −0.55 for **P6**, indicating a more extended spin coupling of **P6**. According to glazing incidence small- and wide-angle X-ray scattering measurements on thin film samples, the π–π distances of **P5** and **P6** are 3.45 Å and 3.51 Å, respectively. These data support the hypothesis that smaller π–π distances lead to larger $|J_{AFM}|$ for these proquinoidal polymers.

For **P7** composed of cyclopentadithiophenyl and thiadiazoloquinoxaline units[76] (Fig. 10a), a paramagnetic ground state was also observed and the singlet–triplet energy gap (ΔE_{S-T}) was calculated to be 9.30×10^{-3} kcal mol^{-1} (Fig. 10b and c) based on superconducting quantum interference device (SQUID) magnetometry results. The triplet ground state, with weak interchain ferromagnetic interaction, was also found to be independent of the spin concentration.

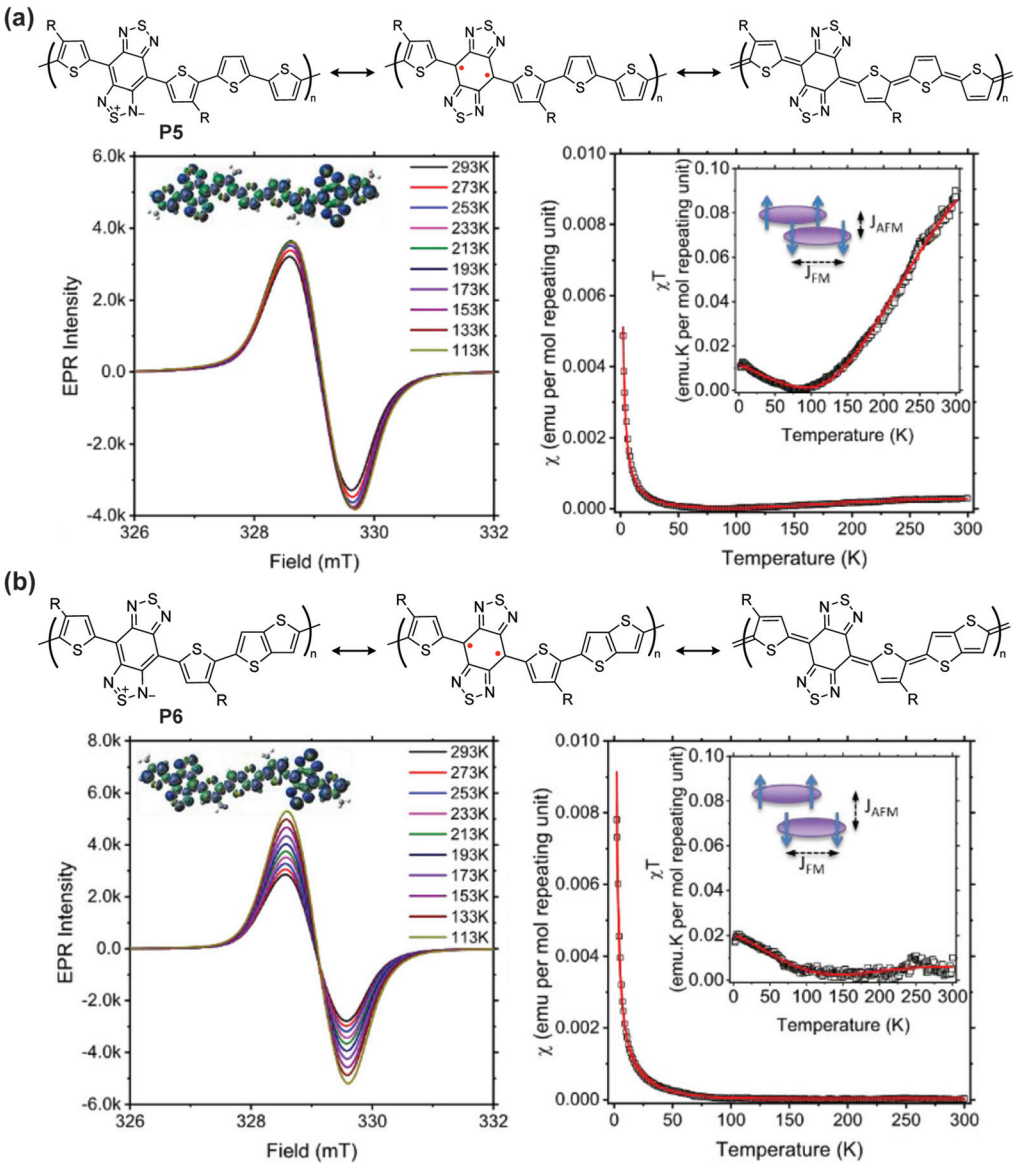

Fig. 9 Closed-shell and open-shell structures of **P5** (a) and **P6** (b), and their variable-temperature-EPR spectra, χ–T and χT–T plots [inset: diagram showing ferromagnetic (FM) and antiferromagnetic (AFM) coupling of spins]. Reproduced from ref. 94 with permission from the American Chemical Society.

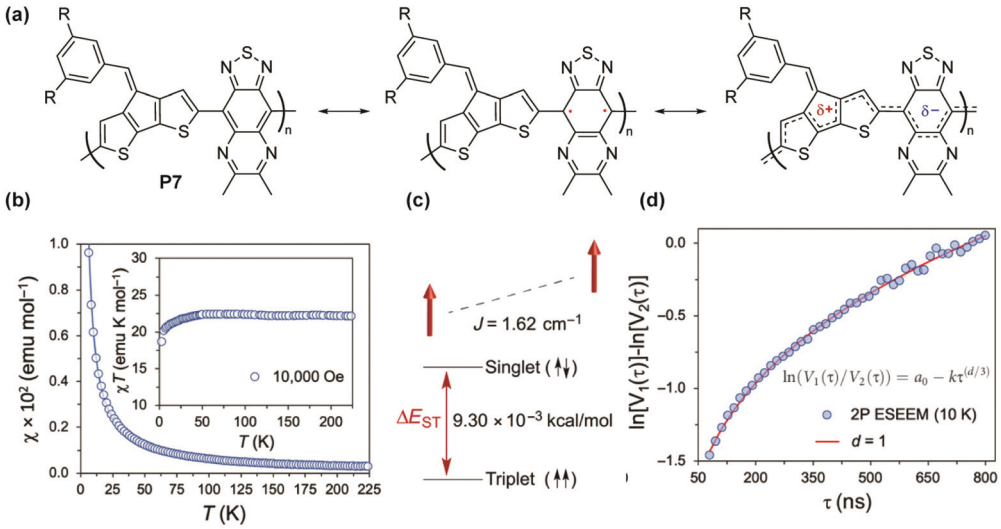

Fig. 10 (a) Closed-shell and open-shell resonance forms of **P7**; (b) χ–T and χT–T plots obtained by SQUID measurement; (c) energy diagram of singlet and triplet states; (d) two-pulse electron spin echo instantaneous diffusion data. Reproduced from ref. 76 with permission from the American Association for the Advancement of Science.

The distribution of spins was characterized by two-pulse spin echo measurements of instantaneous diffusion (Fig. 10d), indicating that the nearest electron spins are approximately distributed in one dimension, as if randomly placed on a linear polymer chain. Similarly, a high spin concentration was also observed for the **P8** series with the triplet ground state and weak ferromagnetic coupling.[77]

Interestingly, the quinoidal–aromatic copolymer **P10** was reported recently as a good singlet fission candidate.[95] The fulfillment of energetic requirements for singlet fission is primarily ascribed to the distinctive biradical character of the heterocyclic quinoidal core.[96,97] **P10** was found to produce long-lived triplet pairs efficiently in strongly coupled polymer thin films, showing the promising potential of quinoidal conjugated polymers in developing next-generation singlet-fission-based organic solar cells.

3.2 Delocalization of polarons/bipolarons

Recently, Wang and coworkers reported[10] direct observation of quinoidal units in PPP chains as charge carriers. Polymers and oligomers were synthesized on the surface of the Cu (111) substrate. The aromatic (benzenoid) and quinoidal forms can be distinctively visualized by scanning tunneling microscopy (STM) and noncontact atomic force microscopy. Most quinoidal segments are found with a length of around 8 rings. The excitation from the ground state aromatic to the quinoidal forms can be facilitated either by a surface adsorption process, which enforces a planar chain conformation, or by the charge transfer from underlying Cu (111). Using STM with a voltage bias, the intrachain transport of quinoidal segments can be observed (Fig. 11a and b). Interchain transport is also directly observed as the quinoidal segment hopped from one chain to

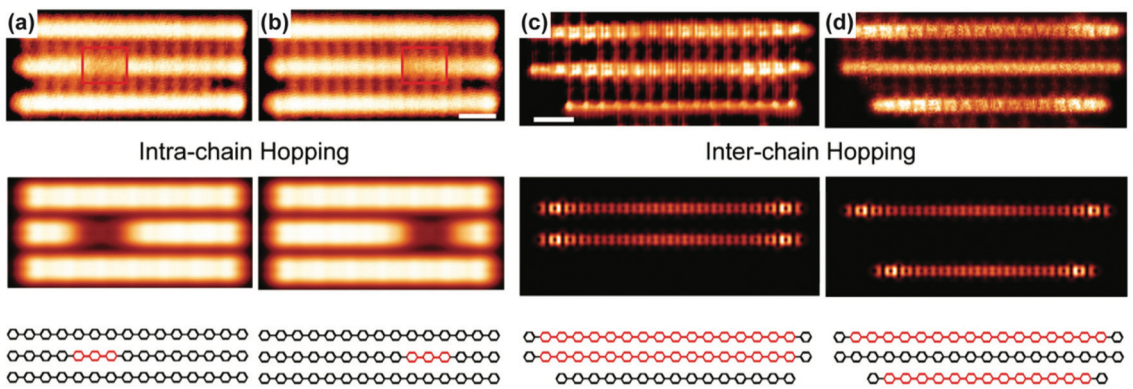

Fig. 11 (a and b) (Top) Experimental STM images of PPP chains showing the transport of the quinoidal segment in one of the chains; (middle) simulated STM images; (bottom) structural representation of the three chains shown above. (c and d) (Top) Constant-height STM images of PPP chains showing the hopping of the quinoidal segment from the middle chain to the bottom chain; (middle) simulated current images; (bottom) structural representation of the three chains shown above. Reproduced from ref. 10 with permission from the American Chemical Society.

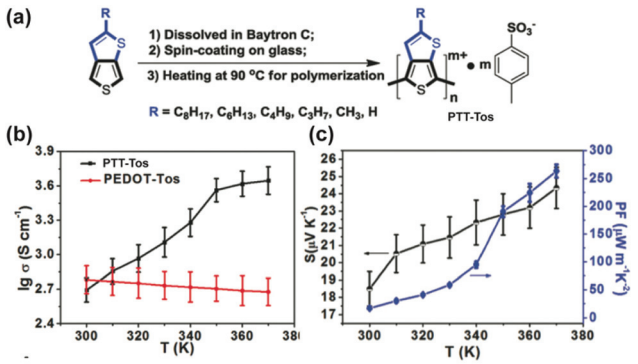

Fig. 12 (a) Synthesis and structural formula of **PTT-Tos**; (b) temperature-dependent conductivity of **PTT-Tos** compared with **PEDOT-Tos**; (c) temperature-dependent Seebeck coefficient and power factor of **PTT-Tos**. Reproduced from ref. 99 with permission from John Wiley and Sons.

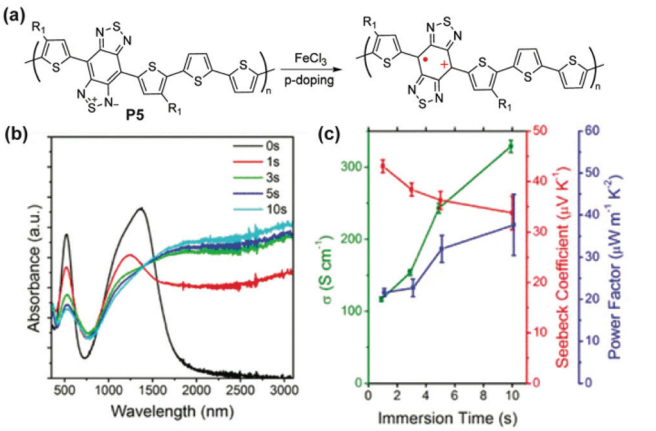

Fig. 13 (a) Structural representation of **P5** before and after oxidative doping; (b) evolution of thin film UV-vis-NIR absorption spectra of **P5** immersed in $FeCl_3$ solution as a function of time; (c) electrical conductivity, Seebeck coefficient, and power factor of **P5** as a function of immersion doping time. Reproduced from ref. 94 with permission from the American Chemical Society.

another (Fig. 11c and d) under a bias of 1 mV. These results suggest a high-mobility character of the quinoidal polarons or bipolarons in PPP on the Cu (111) surface.

The high conductivity rendered by the hopping of quinoidal segment has been applied in organic conducting and thermoelectric devices.[77] For example, the electrical conductivity of up to 6 S cm^{-1} can be achieved on proquinoidal poly(thieno[3,2-*b*] thiophene) (**PTT**).[98] To further enhance the conductivity, Zhu's group developed[99] an *in situ* solution casting polymerization method to prepare doped **PTT-Tos** with tosylate dopant anions (Fig. 12a).[100] The polymer with the shortest alkyl chain (methyl) shows electrical conductivity up to 450 S cm^{-1} at 300 K and 4444 S cm^{-1} at 370 K. Different from the metallic conducting poly(3,4-ethylenedioxythiophene) (PEDOT)-tosylate system, the strong temperature dependence of conductivity indicates a thermally activated hopping mechanism of the transport of quinoidal quasiparticles (Fig. 12b). A polaron-dominant carrier transport mode is proposed based on strong EPR signals. In this work, the increased electrical conductivity at higher temperatures also contributes to the enhanced thermoelectric performances (Fig. 12c).

Other proquinoidal polymers, such as **P5** and **P6**, have also demonstrated promising properties as electrical conducting and thermoelectric materials after doping. After doping with Fe(III), polaron/bipolaron species are generated in **P5** and **P6** (Fig. 13a).[94] With an increased doping level, a broad absorption band spanning from 1000 nm beyond 3100 nm (transition energy lower than 0.4 eV) emerges and increases, suggesting the presence of highly delocalized polarons/bipolarons (Fig. 13b). The electrical conductivities of **P5** and **P6** reach 313.9 S cm^{-1} and 287.0 S cm^{-1} after doping, respectively. The extended intra- and intermolecular delocalization of polarons or bipolarons also renders high Seebeck coefficients *via* carrier-induced softening (46.6 μV $K^{-1}$for **P5** and 65.4 μV K^{-1} for **P6**). The conductivity and the Seebeck coefficient contribute cooperatively in enhancing the thermoelectric power factor up to 43.5 μW m^{-1} K^{-2} for **P5** and 65.2 μW m^{-1} K^{-2} for **P6**. Based on DFT calculation results, the formation of stable triplet bipolarons in doped **P6** is proposed to be the reason for its large Seebeck coefficient despite the high electrical conductivity.

The ladder-type polyaniline analogue **P13c** with quinoidal building blocks can be doped by acid (Fig. 14a) to generate an analogue of pernigraniline salt **P13c-H**. For conventional pernigraniline salt, the iminium bonds are labile under ambient conditions so that the polymer is unstable and cannot be extensively investigated for its intrinsic spin properties, while with a ladder-type constitution, the originally labile iminium linkage is stabilized by the extra strand of bonds.[101] The good stability of **P13c-H** enables the comprehensive study of its strong open-shell character by EPR spectroscopy and SQUID magnetometry (Fig. 14b).[87] The radical cations are delocalized along the ladder-type backbone with extended conjugation. **P13c-H** possesses dominant Pauli paramagnetism and negligible Curie spin character in the solid state (Fig. 14c). The high Pauli paramagnetic susceptibility (χ_{Pauli}) value indicates a significantly enhanced polaron delocalization range, in terms of both intrachain and interchain, and high density of states at the Fermi level.[102]

3.3 Narrowed bandgaps and tunable energy levels

Energy bandgaps of conjugated polymers are determined by a number of factors, including BLA, aromatic resonance energy, substituents, planarity, and intermolecular interactions.[4,103–109] The relationship between energy bandgap and BLA in organic conjugated polymers has been extensively investigated, revealing that quinoidal structures with smaller BLA would efficiently decrease the energy bandgap.[4,5,33,103,104,106–110] Besides the small BLA, another important feature of quinoidal structures is their preferred coplanar conformation. The coplanar conformation can

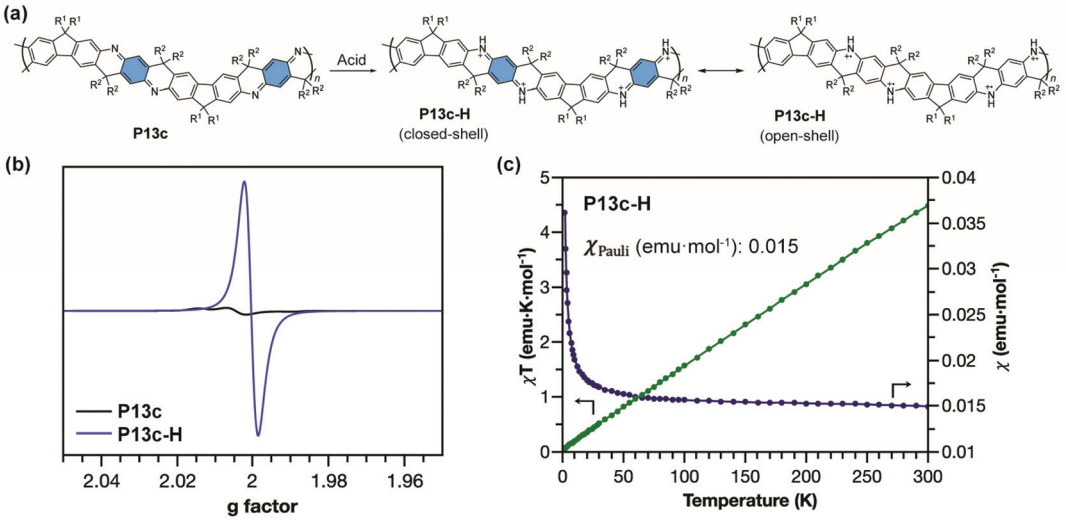

Fig. 14 (a) Structural representation of **P13c** and its acid-doped form **P13c-H** with closed-shell and open-shell resonance structures; (b) EPR spectra of **P13c** and **P13c-H**; (c) χ–T and χT–T plots of **P13c-H** showing dominant Pauli paramagnetism. Reproduced from ref. 87 with permission from the Royal Society of Chemistry.

further lower the energy bandgap[33] by facilitating delocalization of electrons, states, and quasiparticles not only along the backbone but also in between polymer chains through intermolecular electronic coupling. In many cases, quinoidal structures are also the electron-withdrawing units in donor–acceptor systems, leading to intramolecular charge transfer and further reduced energy bandgap. In this context, the quinoidal design has been employed in the development of many conjugated polymer materials for photovoltaic application and field-effect transistors. These examples have been already reviewed in other publications[32,33,35,64,110] so that they are not discussed extensively here. For the polymers covered in this review, their

Table 1 Summary of energy levels and charge mobilities of quinoidal polymers

Ref.	Polymer	E_{HOMO} (eV)	E_{LUMO} (eV)	$E_{g,opt}$ (eV)	μ_h ($cm^2\ V^{-1}\ s^{-1}$)	Device[a]	σ intrinsic ($S\ cm^{-1}$)
111	**P1**	−4.82		1.08	0.0011	BGBC	10^{-2}
	P2	−5.01	−3.60	1.22	0.092		10^{-3}
	P3	−5.02	−3.50	1.26	0.13		10^{-4}
	P4	−5.16	−3.60	1.38			10^{-5}
	P5	−5.06	−3.79	0.70	1.8 (ref. 112)		
	P6	−5.09	−3.84	0.52	1.0 (ref. 113)		
76	**P7**	−4.79	−4.23	<0.30			10^{-2}
77	**P8a**	−4.93	−3.90	0.57	1.75×10^{-1}	BGBC	8.18
	P8b	−5.06	−4.19	0.59	4.50×10^{-4}		2.89×10^{-3}
	P8c	−4.95	−4.15	0.54	1.95×10^{-3}		3.75×10^{-3}
84	**P9a**	−4.90	−3.58	1.32	0.024	BGTC	
	P9b	−5.02	−3.53	1.49	0.47		
	P9c	−5.07	−3.54	1.53	0.082		
95	**P10**			1.78			
85	**P11**	−5.0	−3.6	1.38	0.0039	BGTC	
86	**P12a**	−5.04	−4.11	1.22			
	P12b	−5.07	−4.09	1.33			
87	**P13a**	−4.88		3.10			
	P13b	−4.90	−3.68				
	P13c	−5.33	−3.76	1.57			
91	**P14**			1.81–1.95			
90	**P15**	−5.89 to −5.66	−4.11 to −3.88	1.26–2.07			
92	**P16a**	−5.30	−3.73	1.67			
	P16b	−5.13	−3.70	1.70			
	P16c	−5.06	−3.87	1.59			
	P16d	−5.12	−3.63	1.81			
93	**P17a**	−5.2	−4.0	1.2			
	P17b	−4.9	−3.7	1.2			

[a] BGBC: Bottom-gate/bottom-contact; BGTC: bottom-gate/top-contact.

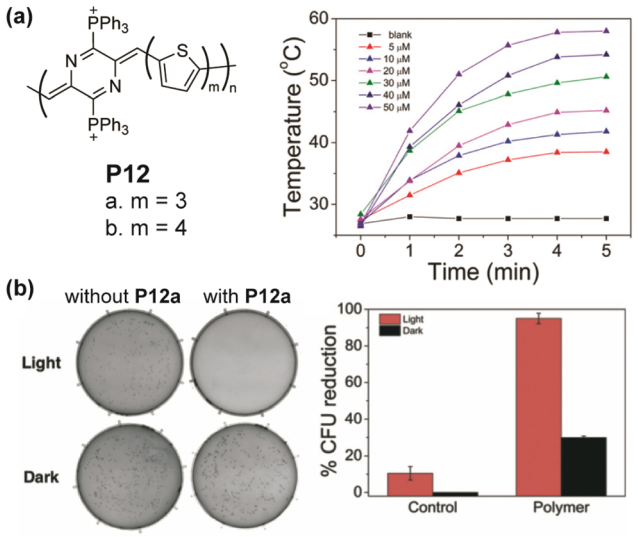

Fig. 15 (a) Structure of **P12** polymers and the photothermal effect of **P12a** in diluted solution; (b) photographs of *S. aureus* colonies with and without **P12a** both with and without 808 nm laser irradiation for 5 min and quantized colony reduction data. Reproduced from ref. 86 with permission from John Wiley and Sons.

parameters and performances associated with these applications are summarized in Table 1.

The low energy bandgap also warrants quinoidal polymers as promising active agents for near-infrared (NIR) photothermal therapy. For example, **P12a** and **P12b** possess NIR absorbance edging at 1010 nm and 940 nm, respectively.[86] Reasonable water solubility of these polymers can be achieved by installing cationic groups on the polymer backbone. In a diluted aqueous solution of **P12b**, a significant photothermal effect is observed. The solution temperature increases to 50.6 °C in 5 min under excitation of an 808 nm laser (Fig. 15a), in drastic contrast with the blank solution. The extent and rate of warming can be controlled and employed to cause the death of bacteria through damage to proteins and lipids on the cell membrane. A 95% reduction of the model bacterial colony is observed after 5 min of irradiation when treated with **P12** solution (Fig. 15b).

4. Conclusion and perspectives

This review summarizes recent advances on the syntheses, properties, and applications of quinoidal conjugated polymers featuring open-shell character. The quinoidal structure imparts a number of intriguing properties—including but not limited to extended π-conjugation, open-shell character, and polaron/bipolaron delocalization—to these polymers. A wide range of polymers with diverse structural constitutions have been investigated to demonstrate great potential as novel high-spin organic materials. However, various challenges still remain in this research topic. First, the scope of structures and syntheses of (pro)quinoidal monomeric building blocks is relatively narrow compared to traditional aromatic conjugated polymers. Although small energy bandgaps have been extensively demonstrated in quinoidal conjugated polymers, studies on their open-shell character are still scarce. Second, it is still challenging to precisely predict and control energy levels of (pro)quinoidal building blocks due to the complex contribution from BLA, intrachain charge transfer, and Peierls distortion.[59] Last but not least, the open-shell character of the quinoidal structure could bring in reactivity and stability issues for fundamental characterization and practical applications.

In future research, the discovery and development of novel quinoidal building blocks and synthetic methodologies are desired in order to achieve precision control of the unique properties of quinoidal conjugated polymers. Further fundamental investigations on the open-shell, high-spin character and polaron and/or bipolaron delocalization properties are critical to understand the nature of quinoidal structures and to render high stability in these materials.

In terms of applications, it is anticipated that quinoidal conjugated polymers will play an impactful role in the future development of organic photovoltaics and field-effect transistors, on the basis of the thriving accomplishments made in these fields and recent progress in singlet fission study. Besides, the incorporation of quinoidal units in doped conjugated polymers can be a viable strategy to achieve robust organic materials with metallic ground states.[77] Last but not least, advances in the understanding of the open-shell character have also enabled the use of quinoidal polymers in organic thermoelectricity, spintronics, nonlinear optics, *etc.*

Conflicts of interest

There are no conflicts to declare.

Acknowledgements

The authors gratefully acknowledge the Robert A. Welch Foundation (A-1898) and the President's Excellence Fund of Texas A&M University (X-Grant) for financial support of this work.

Notes and references

1 IUPAC, *Compendium of Chemical Terminology, 2nd ed. (the "Gold Book")*, Blackwell Scientific Publications, Oxford, 1997.
2 M. Kertesz, C. H. Choi and S. Yang, *Chem. Rev.*, 2005, **105**, 3448.
3 J. Casado, in *Physical Organic Chemistry of Quinodimethanes*, Springer, 2017, pp. 209.
4 S. Rasmussen, in *Encyclopedia of Polymeric Nanomaterials*, ed. S. Kobayashi and K. Müllen, Springer Berlin Heidelberg, Berlin, Heidelberg, 2015, pp. 1155.

5 J. L. Brédas, *J. Chem. Phys.*, 1985, **82**, 3808.
6 N. Bérubé, J. Gaudreau and M. Côté, *Macromolecules*, 2013, **46**, 6873.
7 Y. Hayashi and S. Kawauchi, *Polym. Chem.*, 2019, **10**, 5584.
8 P. M. Burrezo, J. L. Zafra, J. T. López Navarrete and J. Casado, *Angew. Chem., Int. Ed.*, 2017, **56**, 2250.
9 J. Bredas, R. Chance and R. Silbey, *Phys. Rev. B: Condens. Matter Mater. Phys.*, 1982, **26**, 5843.
10 B. Yuan, C. Li, Y. Zhao, O. Gröening, X. Zhou, P. Zhang, D. Guan, Y. Li, H. Zheng, C. Liu, Y. Mai, P. Liu, W. Ji, J. Jia and S. Wang, *J. Am. Chem. Soc.*, 2020, **142**, 10034.
11 T. Y. Gopalakrishna, W. Zeng, X. Lu and J. Wu, *Chem. Commun.*, 2018, **54**, 2186.
12 R. Lv, S. Geng, S. Li, F. Wu, Y. Li, T. R. Andersen, Y. Li, X. Lu, M. Shi and H. Chen, *Solar RRL*, 2020, 2000286.
13 L. Ren, H. Fan, D. Huang, D. Yuan, C. Di and X. Zhu, *Chem. – Eur. J.*, 2016, **22**, 17136.
14 C. Zhang and X. Zhu, *Acc. Chem. Res.*, 2017, **50**, 1342.
15 X. Hu, W. Wang, D. Wang and Y. Zheng, *J. Mater. Chem. C*, 2018, **6**, 11232.
16 D. Huang, H. Yao, Y. Cui, Y. Zou, F. Zhang, C. Wang, H. Shen, W. Jin, J. Zhu, Y. Diao, W. Xu, C. Di and D. Zhu, *J. Am. Chem. Soc.*, 2017, **139**, 13013.
17 J. Casado, R. P. Ortiz and J. T. L. Navarrete, *Chem. Soc. Rev.*, 2012, **41**, 5672.
18 J. Xia, S. N. Sanders, W. Cheng, J. Z. Low, J. Liu, L. M. Campos and T. Sun, *Adv. Mater.*, 2017, **29**, 1601652.
19 C. K. Frederickson, B. D. Rose and M. M. Haley, *Acc. Chem. Res.*, 2017, **50**, 977.
20 T. Stuyver, B. Chen, T. Zeng, P. Geerlings, F. De Proft and R. Hoffmann, *Chem. Rev.*, 2019, **119**, 11291.
21 Y. Li, L. Li, Y. Wu and Y. Li, *J. Phys. Chem. C*, 2017, **121**, 8579.
22 T. Kubo, *Chem. Lett.*, 2015, **44**, 111.
23 J. J. Dressler, M. Teraoka, G. L. Espejo, R. Kishi, S. Takamuku, C. J. Gómez-García, L. N. Zakharov, M. Nakano, J. Casado and M. M. Haley, *Nat. Chem.*, 2018, **10**, 1134.
24 Z. Zeng, X. Shi, C. Chi, J. T. L. Navarrete, J. Casado and J. Wu, *Chem. Soc. Rev.*, 2015, **44**, 6578.
25 W. Zeng, H. Phan, T. S. Herng, T. Y. Gopalakrishna, N. Aratani, Z. Zeng, H. Yamada, J. Ding and J. Wu, *Chem*, 2017, **2**, 81.
26 A. Moliton and R. C. Hiorns, *Polym. Int.*, 2004, **53**, 1397.
27 J. L. Brédas and G. B. Street, *Acc. Chem. Res.*, 1985, **18**, 309.
28 D. Yuan, D. Huang, S. M. Rivero, A. Carreras, C. Zhang, Y. Zou, X. Jiao, C. R. McNeill, X. Zhu, C.-a. Di, D. Zhu, D. Casanova and J. Casado, *Chem*, 2019, **5**, 964.
29 J. Yamamoto and Y. Furukawa, *J. Phys. Chem. B*, 2015, **119**, 4788.
30 A. G. MacDiarmid, *Angew. Chem., Int. Ed.*, 2001, **40**, 2581.
31 J. Scotto, M. I. Florit and D. Posadas, *Electrochim. Acta*, 2018, **268**, 187.
32 T. Mikie and I. Osaka, *J. Mater. Chem. C*, 2020, **8**, 14262.
33 C. Liu, K. Wang, X. Gong and A. J. Heeger, *Chem. Soc. Rev.*, 2016, **45**, 4825.
34 Y. Liang and L. Yu, *Acc. Chem. Res.*, 2010, **43**, 1227.
35 H. Zhou, L. Yang and W. You, *Macromolecules*, 2012, **45**, 607.
36 F. Wudl, M. Kobayashi and A. J. Heeger, *J. Org. Chem.*, 1984, **49**, 3382.
37 I. Hoogmartens, P. Adriaensens, D. Vanderzande, J. Gelan, C. Quattrocchi, R. Lazzaroni and J. L. Brédas, *Macromolecules*, 1992, **25**, 7347.
38 F. Wudl, M. Kobayashi, N. Colaneri, M. Boysel and A. J. Heeger, *Mol. Cryst. Liq. Cryst.*, 1985, **118**, 199.
39 N. Colaneri, M. Kobayashi, A. Heeger and F. Wudl, *Synth. Met.*, 1986, **14**, 45.
40 J. L. Brédas, A. J. Heeger and F. Wudl, *J. Chem. Phys.*, 1986, **85**, 4673.
41 M. Pomerantz, B. Chaloner-Gill, L. O. Harding, J. J. Tseng and W. J. Pomerantz, *J. Chem. Soc., Chem. Commun.*, 1992, 1672.
42 D. D. Kenning and S. C. Rasmussen, *Macromolecules*, 2003, **36**, 6298.
43 L. Wen, B. C. Duck, P. C. Dastoor and S. C. Rasmussen, *Macromolecules*, 2008, **41**, 4576.
44 S. C. Rasmussen, R. L. Schwiderski and M. E. Mulholland, *Chem. Commun.*, 2011, **47**, 11394.
45 Y. Deng, B. Sun, Y. He, J. Quinn, C. Guo and Y. Li, *Angew. Chem., Int. Ed.*, 2016, **55**, 3459.
46 G. A. Sotzing and K. Lee, *Macromolecules*, 2002, **35**, 7281.
47 G. A. Sotzing, V. Seshadri and F. J. Waller, in *Handbook of Conducting Polymer*, ed. T. A. Skotheim and J. R. Reynolds, CRC Press, Boca Raton, 2007, p. 11/1.
48 K. Lee and G. A. Sotzing, *Macromolecules*, 2001, **34**, 5746.
49 J. Kürti, P. R. Surján and M. Kertész, *J. Am. Chem. Soc.*, 1991, **113**, 9865.
50 K. Nayak and D. S. Marynick, *Macromolecules*, 1990, **23**, 2237.
51 C. Arbizzani, M. Catellani, M. Mastragostino and M. Cerroni, *J. Electroanal. Chem.*, 1997, **423**, 23.
52 R. van Asselt, I. Hoogmartens, D. Vanderzande, J. Gelan, P. E. Froehling, M. Aussems, O. Aagaard and R. Schellekens, *Synth. Met.*, 1995, **74**, 65.
53 I. Polec, A. Henckens, L. Goris, M. Nicolas, M. Loi, P. Adriaensens, L. Lutsen, J. Manca, D. Vanderzande and N. Sariciftci, *J. Polym. Sci., Part A: Polym. Chem.*, 2003, **41**, 1034.
54 E. W. Culver, T. E. Anderson, J. T. López Navarrete, M. C. Ruiz Delgado and S. C. Rasmussen, *ACS Macro Lett.*, 2018, **7**, 1215.
55 Y. Zhu, R. D. Champion and S. A. Jenekhe, *Macromolecules*, 2006, **39**, 8712.
56 Y. Liang, D. Feng, Y. Wu, S.-T. Tsai, G. Li, C. Ray and L. Yu, *J. Am. Chem. Soc.*, 2009, **131**, 7792.
57 Y. Liang, Y. Wu, D. Feng, S.-T. Tsai, H.-J. Son, G. Li and L. Yu, *J. Am. Chem. Soc.*, 2009, **131**, 56.
58 J. Hou, H.-Y. Chen, S. Zhang, R. I. Chen, Y. Yang, Y. Wu and G. Li, *J. Am. Chem. Soc.*, 2009, **131**, 15586.

59 N. Kleinhenz, L. Yang, H. Zhou, S. C. Price and W. You, *Macromolecules*, 2011, **44**, 872.
60 T. Zheng, L. Lu, N. E. Jackson, S. J. Lou, L. X. Chen and L. Yu, *Macromolecules*, 2014, **47**, 6252.
61 W. Zhang, T. Huang, J. Li, P. Sun, Y. Wang, W. Shi, W. Han, W. Wang, Q. Fan and W. Huang, *ACS Appl. Mater. Interfaces*, 2019, **11**, 16311.
62 Y. Cai, X. Xue, G. Han, Z. Bi, B. Fan, T. Liu, D. Xie, L. Huo, W. Ma, Y. Yi, C. Yang and Y. Sun, *Chem. Mater.*, 2018, **30**, 319.
63 J. D. Douglas, G. Griffini, T. W. Holcombe, E. P. Young, O. P. Lee, M. S. Chen and J. M. Fréchet, *Macromolecules*, 2012, **45**, 4069.
64 L. Lu, T. Zheng, Q. Wu, A. M. Schneider, D. Zhao and L. Yu, *Chem. Rev.*, 2015, **115**, 12666.
65 H. J. Son, F. He, B. Carsten and L. Yu, *J. Mater. Chem.*, 2011, **21**, 18934.
66 L. Dou, Y. Liu, Z. Hong, G. Li and Y. Yang, *Chem. Rev.*, 2015, **115**, 12633.
67 C. Duan, F. Huang and Y. Cao, *J. Mater. Chem.*, 2012, **22**, 10416.
68 T. L. Tam, H. H. R. Tan, W. Ye, S. G. Mhaisalkar and A. C. Grimsdale, *Org. Lett.*, 2012, **14**, 532.
69 T. L. D. Tam, T. T. Lin and M. H. Chua, *Phys. Chem. Chem. Phys.*, 2017, **19**, 15671.
70 T. L. D. Tam and J. Wu, *J. Mol. Eng. Mater.*, 2015, **3**, 1540003.
71 K. Ono, S. Tanaka and Y. Yamashita, *Angew. Chem., Int. Ed. Engl.*, 1994, **33**, 1977.
72 A. Thomas, K. Bhanuprakash and K. K. Prasad, *J. Phys. Org. Chem.*, 2011, **24**, 821.
73 A. Thomas and K. Bhanuprakash, *ChemPhysChem*, 2012, **13**, 597.
74 A. Thomas, G. Krishna Chaitanya, K. Bhanuprakash and K. M. M. Krishna Prasad, *ChemPhysChem*, 2011, **12**, 3458.
75 J. D. Yuen, R. Kumar, D. Zakhidov, J. Seifter, B. Lim, A. J. Heeger and F. Wudl, *Adv. Mater.*, 2011, **23**, 3780.
76 A. E. London, H. Chen, M. A. Sabuj, J. Tropp, M. Saghayezhian, N. Eedugurala, B. Zhang, Y. Liu, X. Gu, B. Wong, N. Rai, M. K. Bowman and J. D. Azoulay, *Sci. Adv.*, 2019, **5**, eaav2336.
77 L. Huang, N. Eedugurala, A. Benasco, S. Zhang, K. S. Mayer, D. J. Adams, B. Fowler, M. M. Lockart, M. Saghayezhian, H. Tahir, E. R. King, S. Morgan, M. K. Bowman, X. Gu and J. D. Azoulay, *Adv. Funct. Mater.*, 2020, **30**, 1909805.
78 I. Osaka, T. Abe, H. Mori, M. Saito, N. Takemura, T. Koganezawa and K. Takimiya, *J. Mater. Chem. C*, 2014, **2**, 2307.
79 K. Kawabata, M. Saito, I. Osaka and K. Takimiya, *J. Am. Chem. Soc.*, 2016, **138**, 7725.
80 W. Hong, C. Guo, Y. Li, Y. Zheng, C. Huang, S. Lu and A. Facchetti, *J. Mater. Chem.*, 2012, **22**, 22282.
81 P. Deng, L. Liu, S. Ren, H. Li and Q. Zhang, *Chem. Commun.*, 2012, **48**, 6960.
82 W. Yue, X. Huang, J. Yuan, W. Ma, F. C. Krebs and D. Yu, *J. Mater. Chem. A*, 2013, **1**, 10116.
83 G. W. van Pruissen, E. A. Pidko, M. M. Wienk and R. A. Janssen, *J. Mater. Chem. C*, 2014, **2**, 731.
84 X. Liu, B. He, C. L. Anderson, J. Kang, T. Chen, J. Chen, S. Feng, L. Zhang, M. A. Kolaczkowski, S. J. Teat, M. A. Brady, C. Zhu, L.-W. Wang and Y. Liu, *J. Am. Chem. Soc.*, 2017, **139**, 8355.
85 X. Liu, B. He, A. Garzón–Ruiz, A. Navarro, T. L. Chen, M. A. Kolaczkowski, S. Feng, L. Zhang, C. A. Anderson, J. Chen and Y. Liu, *Adv. Funct. Mater.*, 2018, **28**, 1801874.
86 C. L. Anderson, N. Dai, S. J. Teat, B. He, S. Wang and Y. Liu, *Angew. Chem.*, 2019, **58**, 17978.
87 X. Ji, M. Leng, H. Xie, C. Wang, K. R. Dunbar, Y. Zou and L. Fang, *Chem. Sci.*, 2020, **11**, 12737.
88 Y. Zou, X. Ji, J. Cai, T. Yuan, D. J. Stanton, Y.-H. Lin, M. Naraghi and L. Fang, *Chem*, 2017, **2**, 139.
89 W.-C. Chen and S. A. Jenekhe, *Macromolecules*, 1995, **28**, 454.
90 Q. Zhang, J. Feng, K. Liu, D. Zhu, M. Yang, H. Ye and X. Liu, *Synth. Met.*, 2006, **156**, 804.
91 J. Li, C. Lai, X. Jia, L. Wang, X. Xiang, C.-L. Ho, H. Li and W.-Y. Wong, *Composites, Part B*, 2015, **77**, 248.
92 K. Peng, T. Pei, N. Huang, L. Yuan, X. Liu and J. Xia, *J. Polym. Sci., Part A: Polym. Chem.*, 2018, **56**, 1676.
93 T. Umeyama, Y. Watanabe, M. Oodoi, D. Evgenia, T. Shishido and H. Imahori, *J. Mater. Chem.*, 2012, **22**, 24394.
94 T. L. Tam, G. Wu, S. W. Chien, S. F. V. Lim, S.-W. Yang and J. Xu, *ACS Mater. Lett.*, 2020, **2**, 147.
95 L. Wang, X. Liu, X. Shi, C. L. Anderson, L. M. Klivansky, Y. Liu, Y. Wu, J. Chen, J. Yao and H. Fu, *J. Am. Chem. Soc.*, 2020, **142**, 17892.
96 M. B. Smith and J. Michl, *Chem. Rev.*, 2010, **110**, 6891.
97 Z. Sun, Z. Zeng and J. Wu, *Acc. Chem. Res.*, 2014, **47**, 2582.
98 A. Patra, Y. H. Wijsboom, G. Leitus and M. Bendikov, *Chem. Mater.*, 2011, **23**, 896.
99 D. Yuan, L. Liu, X. Jiao, Y. Zou, C. R. McNeill, W. Xu, X. Zhu and D. Zhu, *Adv. Sci.*, 2018, **5**, 1800947.
100 O. Bubnova, Z. U. Khan, A. Malti, S. Braun, M. Fahlman, M. Berggren and X. Crispin, *Nat. Mater.*, 2011, **10**, 429.
101 X. Ji, H. Xie, C. Zhu, Y. Zou, A. U. Mu, M. Al-Hashimi, K. R. Dunbar and L. Fang, *J. Am. Chem. Soc.*, 2020, **142**, 641.
102 V. Krinichnyi, A. Konkin and A. Monkman, *Synth. Met.*, 2012, **162**, 1147.
103 S. Rasmussen, K. Ogawa and S. Rothstein, in *Handbook of Organic Electronics and PhotonicsAmerican Scientific Publishers*, ed. H. S. Nalwa, American Scientific Publishers, Stevenson Ranch, CA, 2008, vol. 1, p. 1.
104 J. Roncali, *Chem. Rev.*, 1997, **97**, 173.
105 H. A. M. v. Mullekom, J. A. J. M. Vekemans, E. E. Havinga and E. W. Meijer, *Mater. Sci. Eng., R*, 2001, **32**, 1.
106 J. Roncali, *Macromol. Rapid Commun.*, 2007, **28**, 1761.
107 S. Rasmussen and M. Pomerantz, in *Handbook of Conducting Polymers*, ed. T. A. Skotheim and

J. R. Reynolds, CRC Press, Boca Raton, FL, 3rd edn, 2007, p. 12/1.
108 C. L. Chochos and S. A. Choulis, *Prog. Polym. Sci.*, 2011, **36**, 1326.
109 E. Bundgaard and F. C. Krebs, *Sol. Energy Mater. Sol. Cells*, 2007, **91**, 954.
110 H. J. Jhuo, P. N. Yeh, S. H. Liao, Y. L. Li, Y. S. Cheng and S. A. Chen, *J. Chin. Chem. Soc.*, 2014, **61**, 115.
111 T. L. Tam, C. K. Ng, S. L. Lim, E. Yildirim, J. Ko, W. L. Leong, S.-W. Yang and J. Xu, *Chem. Mater.*, 2019, **31**, 8543.
112 J. Fan, J. D. Yuen, W. Cui, J. Seifter, A. R. Mohebbi, M. Wang, H. Zhou, A. J. Heeger and F. Wudl, *Adv. Mater.*, 2012, **24**, 6164.
113 J. Fan, J. D. Yuen, M. Wang, J. Seifter, J. H. Seo, A. R. Mohebbi, D. Zakhidov, A. Heeger and F. Wudl, *Adv. Mater.*, 2012, **24**, 2186.